

1 Assimilation of SCIAMACHY total column CO
2 observations: Regional analysis of data impact

Andrew Tangborn*, Ivanka Stajner*[†], Michael Buchwitz[‡], Iryna Khlystova[‡],

3 Steven Pawson*, John Burrows[‡], Rynda Hudman[§] and Philippe Nedelec[¶]

4 July 15, 2008

*Global Modeling and Assimilation Office, Goddard Space Flight Center, Greenbelt, MD

[†]Now at Noblis, Falls Church, VA

[‡]Institute of Environmental Physics, University of Bremen, FB1, Bremen, Germany

[§]Atmospheric Chemistry Modeling Group, Harvard University, Cambridge, MA, USA

[¶]Université de Toulouse, Laboratoire d'Aérodynamique, CNRS UMR, Toulouse, France

5 Abstract

6 Carbon monoxide (CO) total column observations from the SCanning Imaging Absorption
7 SpectroMeter for Atmospheric CHartographY (SCIAMACHY) on board ENVISAT are assimi-
8 lated into the Global Modeling and Assimilation Office (GMAO) constituent assimilation system
9 for the period July 18-October 31, 2004. This is the first assimilation of CO observations from a
10 near infrared sounder. The impact of the assimilation on CO distribution is evaluated using in-
11 dependent Measurement of Ozone and Water Vapor by Airbus In-service Aircraft (MOZAIC) *in*
12 *situ* CO profiles. Assimilation of satellite data improves agreement with MOZAIC CO globally,
13 especially in the upper troposphere. Regional comparisons are made in western Europe, the
14 northeastern United States and the Arabian Peninsula. SCIAMACHY assimilation improves
15 CO mixing ratios at pressures ≤ 800 hPa in all three locations. In contrast, the only substan-
16 tial planetary boundary layer improvements occur over the Arabian Peninsula, with mean error
17 reduction of 50%.

18 Model errors (sources and chemistry) are investigated through experiments with increased
19 surface CO emissions over the Arabian Peninsula and/or globally reduced hydroxyl radical (OH)
20 concentrations. Both model changes decrease mean errors at all altitudes in the free running
21 model in comparison to MOZAIC data over Dubai and Abu Dhabi. In contrast, errors in the
22 assimilated CO are reduced by the increased emissions only near the ground for pressures \geq
23 800 hPa and by the reduced OH only for pressure ≤ 600 hPa. Our analysis suggests that
24 CO emissions over Dubai in 2004 are more than 100% larger than those in the 1998 emissions
25 inventory.

1 Introduction

Carbon monoxide (CO) is an important atmospheric trace gas for the global carbon cycle and air quality. The two largest sources of CO, biomass burning and fossil fuel combustion, are also important sources of carbon dioxide (CO₂). CO impacts the air quality directly and as a precursor to tropospheric ozone. Several satellite missions carry instruments that measure radiances at wavelengths sensitive to CO, including the Atmospheric Infrared Sounder (AIRS) [McMillan *et al.*, 2005], Measurements of Pollution in the Troposphere (MOPITT) [Deeter *et al.*, 2003] and the Scanning Imaging Absorption Spectrometer for Atmospheric Chartography (SCIAMACHY) [Buchwitz *et al.*, 2007]. Infrared AIRS and MOPITT radiances are most sensitive to CO between pressures of 400 and 700 hPa. SCIAMACHY CO is retrieved from reflected solar radiation in the near infrared band 2324-2335 nm, which is sensitive to variations within the boundary layer. This is an important distinction for air quality and source inversion applications.

Chemical constituent data assimilation involves combining observations with model forecasts in order to improve estimation of the constituent distribution or sources (in the case of chemical inversion). Assimilation provides a useful tool to evaluate the accuracy of retrieved satellite data relative to models or other measurements. Total column measurements cannot be directly compared with *in situ* point observations without a knowledge of the complete atmospheric profile. Three-dimensional analyzed constituent fields can provide a transfer standard [Lahoz *et al.*, 2007] for indirect comparisons since they can be judged against both the total column and *in situ* observations. If the analysis fields are drawn closer to highly accurate independent data as a result of assimilating satellite observations, this gives a strong indication that the latter provide useful information. When direct measurements of CO profiles are available, the correction made through assimilating total column observations from a satellite can then be evaluated in terms of whether CO is added (or removed) in the appropriate model level.

In this paper we assess the impact of SCIAMACHY total column CO observations on the CO assimilation system developed at the Global Modeling and Assimilation Office (GMAO). This system uses meteorological analyses from the Goddard Earth Observing System (GEOS), Version 4 [Bloom *et al.*, 2005], [Stajner *et al.*, 2008]. The assimilation is evaluated using *in situ* observations from the Measurement of Ozone, water vapor, carbon monoxide and nitrogen oxides by Airbus in-service airCraft (MOZAIC) observing system [Nedelec, *et al.*, 2003]. We investigate where SCIAMACHY observations can make the greatest improvements to CO estimation, and what information the assimilation and comparisons with *in situ* data can provide about the source of errors in the model. The assimilation system is run for the period July 18 - October

59 31, 2004. The comparison with MOZAIC data is done during September and October.

60 2 SCIAMACHY Observations

61 The SCIAMACHY instrument has been operating on board the environmental satellite, EN-
62 VISAT, of the European Space Agency (ESA) since March 2002. The SCIAMACHY observtions
63 exhibit seasonal variability expected in global CO fields [Buchwitz *et al*, 2007]. Figure 1 shows
64 3 month averaged total column CO from SCIAMACHY for the year 2004. These indicate
65 hemispheric differences and large scale seasonal patterns, such as biomass burning over South
66 America and Africa, which are qualitatively consistent with MOPITT observations [Bremer *et*
67 *al*, 2004]. Data assimilation, on the other hand, can determine whether the observations include
68 any useful information on the vertical structure of the CO fields.

69 Retrievals of total column CO (denoted c_{tc}^o) use the Weighting Function Modified - Differen-
70 tial Optical Absorption Spectroscopy (WFM-DOAS) algorithm. WFM-DOAS is a least squares
71 technique that uses the scaling and shifting of pre-selected vertical profiles to fit the ratio of the
72 measured nadir radiance to the solar irradiance spectrum [Buchwitz *et al.*, 2007]. This approach
73 is valid only for cloud free pixels, and a cloud detection algorithm using sub-pixel information
74 generates a cloud mask. The SCIAMACHY c_{tc}^o observations are supplied with a cloud con-
75 tamination flag, as well as a quality flag, which depends on the magnitude of the residual of
76 the least squares fit for each retrieval. The estimated observation error for each total column
77 measurement, σ^{scia} , is calculated from the RMS of the residual and contains contributions from
78 both random and (unknown) systematic components. These total error values generally range
79 from 20% to 100% for the observations tagged as “good”. Only the cloud free “good” quality
80 data are used in the assimilation.

81 The sensitivity of measured radiation to variations in CO at different levels in the atmosphere
82 is characterized by the vertical column averaging kernels, shown in Figure 2(a). For a given solar
83 zenith angle (SZA) the curve represents the sensitivity of the retrievals to changes in CO at each
84 level. Only data for $SZA < 75^\circ$, whose averaging kernels very close to unity, are assimilated.
85 Note that there is slightly more sensitivity to concentrations near 200 hPa than in the lower
86 Troposphere and that the near-surface sensitivity decreases as solar zenith angle increases. There
87 is also some dependence of the averaging kernel on surface reflectivity, which tends to be higher
88 over land than water.

89 The SCIAMACHY observtions exhibit seasonal variability expected in global CO fields
90 [Buchwitz *et al*, 2007] Figure 1 shows 3 month averaged total column CO from SCIAMACHY

91 for the year 2004. These indicate hemispheric differences and large scale seasonal patterns, such
 92 as biomass burning over South America and Africa, which are qualitatively consistent with MO-
 93 PITT observations [Bremer *et al.*, 2004]. Data assimilation, on the other hand, can determine
 94 whether the observations include any useful information on the vertical structure of the CO
 95 fields.

96 3 Assimilation system

97 .

The CO assimilation system used here is based on the ozone assimilation system developed at NASA/Goddard [Stajner *et al.*, 2001,2008] and employs the sequential Physical-space Statistical Analysis System (PSAS) [Cohn *et al.*, 1998], which is an alternative formulation of 3DVAR. The CO data assimilation system has the capability to include the effect of the averaging kernel, which takes into account vertical variations of the sensitivity of the retrieved to actual CO mixing ratios. Because we limit the observations to those with the averaging kernels near unity, the forward (or observation) operator from model space to total column observation space simply involves integrating vertically across each of the pressure layers, multiplying by a constant conversion factor. The *a priori* profile that was used in SCIAMACHY retrievals is subtracted out within each layer, and the total column *a priori* is added to the final result. For a profile \mathbf{x} given on $N = 55$ model levels by mixing ratios $x_k, k = 1, \dots, N$ in kg/kg , we introduce the linear operator $H(x)$

$$H(\mathbf{x}) = \sum_{k=1}^N a_k(\Delta P_k) 2.12 \times 10^{22} x_k. \quad (1)$$

where a_k is the SCIAMACHY averaging kernel, ΔP_k is the k^{th} layer pressure thickness (hPa). The constant (2.12×10^{22}) converts the total column value to *molecules/cm²*. In our application $a_k = 1$. The total column operator that computes the total column CO in *molecules/cm²* is

$$\mathcal{H}(\mathbf{x}) = H(\mathbf{x} - \mathbf{x}^{ap}) + c_{tc}^{ap}, \quad (2)$$

98 where \mathbf{x}^{ap} is the *a priori* CO mixing ratio on model levels and c_{tc}^{ap} is the total column *a priori*.

Eq. (2) defines the observation operator that allows for the calculation of the observed minus forecast (O-F) values in observation space needed for the assimilation system. The PSAS algorithm solves the innovation equation

$$\left(\mathbf{H} \mathbf{P}^f \mathbf{H}^T + \mathbf{R} \right) \mathbf{y} = \left(\mathbf{c}_{tc}^o - \mathcal{H}(\mathbf{x}^f) \right) \quad (3)$$

for the vector \mathbf{y} , in observation space. Here \mathbf{x}^f is the forecast CO mixing ratio kg/kg . The observation operator, \mathbf{H} , is the matrix form of the linear operator in (1) and error statistics

are represented by the forecast error covariance, \mathbf{P}^f . The observation error covariance, \mathbf{R} is a diagonal matrix with with observation error variances on the diagonal, implying that the observation errors are uncorrelated. The solution is then transformed to model space via

$$\mathbf{x}^a - \mathbf{x}^f = \mathbf{P}^f \mathbf{H}^T \mathbf{y} \quad (4)$$

99 to obtain the analysis increment $\mathbf{x}^a - \mathbf{x}^f$, where \mathbf{x}^a is the CO analysis and \mathbf{x}^f is the CO forecast.

The forecast error covariance is specified using a separable covariance model

$$\{P_{i,j}\} = \sigma_i \sigma_j \rho_{i,j} \mu_{i,j}, \quad (5)$$

100 where $\{P_{i,j}\}$ is the covariance between locations i and j , σ_i and σ_j are the forecast error stan-
 101 dard deviations, $\rho_{i,j}$ is a non-isotropic horizontal error correlation and $\mu_{i,j}$ is the vertical error
 102 correlation. Stajner *et al.* [2001] give further details on this background error covariance model.
 103 Three tunable parameters are used in the error covariance models: α specifies the forecast error
 104 standard deviation as a fraction of the local CO mixing ratio, $\sigma^f = \alpha \mathbf{x}^f$, L is the background
 105 error correlation length scale, and β is used to specify observation error standard deviation
 106 $\sigma^o = \beta \sigma^{scia}$. Tuning runs covering the period July 18th to October 31st 2004 determined the
 107 following optimal values: $\alpha = 0.2$ and $\beta = 0.5$. The optimal horizontal correlation length scale
 108 (as determined by minimizing the RMS difference with MOZAIC observations) was found to
 109 be 100 km in the meridional direction, and varies from 200 km in the tropics to 100 km in
 110 high latitudes for the zonal direction. These parameter values are used in all the assimilation
 111 experiments presented in the next section. The value of β implies that the observation errors
 112 provided with the CO retrievals are too large (relative to the MOZAIC observations), possibly
 113 due to an overestimation of the systematic component of the error.

114 The CO forecasts are produced on-line in the GEOS-4 GCM, with linearized chemistry and
 115 imposed sources. The GCM uses the semi-Lagrangian transport finite volume scheme [Lin, 2004]
 116 with 55 levels between the surface and 0.1 hPa. The meteorological analyses are generated using
 117 the GEOS-4 assimilation system [Bloom, *et al.*, 2005], and are then utilized for 6-hour GCM
 118 runs which drive the constituent transport. Meteorological and constituent fields are computed
 119 on a 1 deg latitude by 1.25 deg longitude grid. The model is employed in two ways. First,
 120 it is used to produce a CO simulation, in which CO transport is constrained by the GEOS-4
 121 meteorological analyses. This run is called the ‘‘CO simulation’’. Second, it is used to forecast
 122 CO (provide the background fields) for the ‘‘CO assimilation’’, in which the SCIAMACHY
 123 observations are inserted every six hours to provide new initial conditions (analyses). Transport
 124 fields are identical in both runs.

The CO production (P) rate and loss (L) frequencies are taken from the GEOS-CHEM model [Wang *et al.*, 1998; Bey *et al.*, 2001] and a specific description of the coupled oxidant-aerosol simulation as used in that version of the model is given by Park *et al.* [2004]. Monthly mean climatological hydroxyl radical (OH) concentration is used to specify CO destruction. The net rate of change in CO mixing ratio on the model grid is then

$$\frac{\partial[CO]}{\partial t} = P - L[OH][CO]. \quad (6)$$

125 We use a global anthropogenic emissions inventory for 1998 as described in Bey *et al.* [2001].
126 Anthropogenic emissions over the United States are from the 1999 National Emission Inventory
127 (NEI) with modifications described by Hudman *et al.* [2007], including a generalized 50% de-
128 crease in *NOx* emissions from power plants and industry reflecting documented changes between
129 1999-2004, and a 30% decrease in *CO* emissions to account for overestimate in the transport
130 sector [Parrish, 2006]. Biogenic emissions of isoprene and monoterpenes are from the Global
131 Emissions Inventory Activity (GEIA) [Guenther *et al.*, 1995]. We assume an instantaneous
132 monoterpene yield of 0.2 CO per atom C [Duncan *et al.*, 2007]. Biogenic alkene ($C \geq 3$) emis-
133 sions are assumed to be 10% of isoprene on a per molecule basis. Biogenic acetone emissions
134 are as in Jacob *et al.*, [2002]. Biofuel emissions are as described in Yevich and Logan [2003].
135 Biomass burning emissions are climatological means as described in Duncan *et al.* [2003], with
136 the addition of fire emissions over North America following Turquety *et al.* [2007], and we as-
137 sume that 40% of the biomass burning emissions are released at the surface and 60% are released
138 in the free troposphere.

139 4 Assimilation results

140 The impact of SCIAMACHY data for a single analysis time can be seen in Figure 2(b) in a
141 vertical slice of the analysis increment (analysis minus forecast) at 25° E and 18UT on September
142 30, 2004. This increment includes a number of observations, and the most substantial corrections
143 correspond to three observations in or near the plane of this plot. The corrections continue all
144 the way to the surface where they reach a maximum. This vertical structure is due to the
145 assumption that the forecast error standard deviation is proportional to the local CO mixing
146 ratio, which is typically highest in the boundary layer. The shape of the SCIAMACHY analysis
147 increments contrasts with the shape of MOPITT increments, which tend to peak around 500
148 mb, and then decay toward the surface [Lamarque *et al.*, 2004].

149 Global and regional comparisons with MOZAIC observations are used to evaluate model per-
150 formance and impact of SCIAMACHY data. Regional comparisons focus on three 10° latitude

151 $\times 10^\circ$ longitude boxes centered near Frankfurt, Germany; New York, USA; and Dubai, UAE.
152 Separating the comparisons with independent data in this manner allows us to consider the
153 impact of the geographic variability of the accuracy of the source estimates on the assimilation.
154 Jet takeoffs and landings in each region provide CO profiles numbering from around 12 (Dubai
155 and Abu Dhabi) to about 150 (Frankfurt) from near sea level to about 200 mb for the period
156 from September 1 to October 31, 2004. Note that the nature of MOZAIC observations means
157 that spatial coverage and temporal sampling have large geographical differences [Nedelec, *et al.*
158 1998].

159 Global comparisons of the mean and root-mean-square (RMS) differences between MOZAIC
160 observations the CO simulation (not shown) reveal that CO values in the model are generally
161 too low at pressures lower than 700 hPa. At higher pressures the model errors are much more
162 dependent on geographical location, and for this reason we are concerned with a more localized
163 comparison. Figures 3 - 5 show the relative mean and RMS of the difference between the
164 MOZAIC observations and the CO simulation (solid) or CO analyses (dash-dot) interpolated
165 to the MOZAIC observation locations within the boxes centered on Frankfurt, Dubai and New
166 York City, respectively. Profiles over Dubai show larger errors than over New York or Frankfurt.
167 Assimilation of SCIAMACHY data provides closer agreement with MOZAIC CO globally (not
168 shown). The improvement is particularly large near Dubai, where larger analysis increments
169 counteract large model errors. For example, the mean error reduction above Dubai varies from
170 50% at the surface to 100% just above the boundary layer. In contrast, the mean errors near
171 Frankfurt and New York are essentially unchanged by the assimilation in the surface layer. Note
172 that the mean error in the upper troposphere is substantially reduced by the assimilation over
173 all three cities.

174 Similarly, the RMS errors show a reduction at all levels only over Dubai, where the decrease
175 varies from 10% at the surface to about 50% in the upper troposphere. Above New York
176 and Frankfurt, reduction occurs only at pressures below 900 hPa, with a maximum reduction of
177 about 30%. In all three locations, and for pressures lower than 900 hPa, the analysis RMS errors
178 vary from 15% to 30%. The forecast RMS errors (not shown) are very similar in magnitude
179 to the analysis RMS errors, indicating that the estimated forecast error of 20% of the CO
180 mixing ratio is reasonable outside the boundary layer. contain information on upper troposphere
181 CO. Over Dubai, assimilation of SCIAMACHY data decreases mean and RMS differences with
182 MOZAIC data in the boundary layer. Over the Arabian Peninsula, favorable conditions for the
183 assimilation include the frequent availability of cloud-free SCIAMACHY data and the fact that

184 the model is consistently too low in the boundary layer and in the total columns. The former
185 allows frequent corrections due to the assimilation and the latter ensures that the distribution of
186 analysis increments in the vertical helps improve the representation of CO in the boundary layer.
187 Assimilation of SCIAMACHY data leads to a consistent large decrease in the RMS differences
188 with MOZAIC data globally and in the three regions between about 200 and 700 hPa. At these
189 levels, which are away from the immediate impact of errors in CO sources, the impact of the
190 analysis increments can accumulate to produce these substantial corrections.

191 The impact of the assimilation of SCIAMACHY as a function of pressure can be seen in
192 Figure 6, which shows the difference between the CO analyses and CO simulation (A-M) aver-
193 aged over September and October 2004 for the three regions studied. Each plot is for a vertical
194 slice from the surface to 200 hPa at a latitude that runs through Frankfurt (a), Dubai (b) or
195 New York (c). In the Frankfurt and New York regions, the correction is largest at pressures
196 lower than 800 hPa, with little or no correction near the surface. Since the analysis increments
197 from the assimilated SCIAMACHY observations will generally correct the entire columns in the
198 same direction [Figure 2(b)], this means that the changes made in the upper troposphere CO
199 are the result of corrections made elsewhere and transported to these regions. For example,
200 the upper level increase in CO over New York appears to be transported from the west, where
201 larger positive corrections to CO were made. The very small or even negative changes nearer
202 the surface can be attributed to some combination of a more accurate emissions model, and
203 a relatively small number of cloud free observations. Similar arguments can be made for the
204 Frankfurt region. Above Dubai the assimilation changes the CO field in a much different way;
205 the corrections are positive right down to the surface, and gives the appearance of “plumes”
206 above Riyadh and Dubai. These are really corrections to rising plumes of CO over the two cities,
207 and they indicate that the specified CO sources are too small in this region.

208 Because assimilation of SCIAMACHY CO results in correction to the entire plume, it is
209 interesting to plot the surface layer CO fields in the Arabian Peninsula. Figure 7 shows the
210 average fields for September-October 2004 in this region. The assimilation increases surface
211 layer CO throughout the peninsula. This indicates a substantial underestimation of CO surface
212 layer concentration in the model. In particular the concentrations around the two largest sources,
213 Kuwait city and Jeddah, increase substantially. The only two cities with MOZAIC data in the
214 Arabian Peninsula region during this time period are Dubai and Abu Dhabi, and there the
215 increase in CO due to the assimilation improves the agreement with MOZAIC data (Figure
216 4). Two possible causes for low bias in the model are considered: underestimated CO surface

217 sources and overestimated CO loss due to its reaction with OH aloft.

218 Additional experiments provide insight on how the model and assimilation respond to changes
219 in emissions and/or OH concentrations. Doubling the CO emissions in the Arabian Peninsula
220 increased CO (and reduced errors) at all levels in the free running model, but only for pressures
221 above 800 mb in the assimilation. Similarly a global 10% reduction in OH reduced errors at all
222 levels in the free running model, but only upper tropospheric errors ($p < 600$ hPa) were reduced
223 in the assimilation. We show the mean errors with and without these changes to emission and
224 global OH in Figure 8. Combining increased Arabian emission with a global 10% decrease in
225 OH provides the best agreement with MOZAIC data for both the model and the assimilation.
226 At the surface in Dubai, doubled regional emissions and globally 10% reduced OH decrease the
227 mean error in comparison with MOZAIC by about 30% (from 0.39 to 0.27 ppmv). Note that
228 the assimilation of SCIAMACHY data into this model further reduces the error by about 50%
229 (from 0.27 to 0.13 ppmv). This relative error reduction is very similar to the improvement from
230 assimilation of SCIAMACHY into the original model.

231 The spatial impact of these changes to the chemistry model can be seen in Figure 9, which
232 shows the total column differences between SCIAMACHY observations and model simulations
233 averaged over the month of October 2004, using standard chemistry (Figure 9a) and chemistry
234 with doubled Middle East emissions and OH reduced globally by 10% (Figure 9b). These plots
235 indicate that the higher levels of CO that result from this enhanced chemistry draw the total
236 column CO closer to SCIAMACHY observations. For example in the region near Dubai and Abu
237 Dhabi (where the MOZAIC profile measurements are made), the total column differences are
238 reduced from about 1.0×10^{18} to about 0.6×10^{18} . Total column O-F values for the assimilation
239 run using both the original and enhanced chemistry (not shown) are smaller than those in Figure
240 9 and show little dependence on the chemistry model used. This is due to the fact that the
241 assimilation draws the CO total columns strongly towards the observed values.

242 5 Concluding Remarks

243 The assimilation of SCIAMACHY total column CO observations is found to draw the CO
244 analyses closer to an independent data set both globally and in the localized regions of the
245 northeastern United States, the Arabian Peninsula and Western Europe. The mean CO mixing
246 ratio is drawn toward MOZAIC profiles from 200 mb down to the surface. RMS differences with
247 MOZAIC are also substantially reduced by the assimilation, though error reduction from the
248 surface to the 850 mb level is less consistent. We conclude that SCIAMACHY observations are

249 most useful in regions with frequent cloud free days, and particularly when the CO production
250 in the model is less accurate. For example, mean surface errors over Dubai were reduced by
251 about 50%. The observations have less impact in regions with more accurate CO sources or
252 with fewer cloud-free SCIAMACHY observations. The RMS errors in the assimilation show
253 that the assumption of a forecast error standard deviation of about 20% is justifiable in the
254 free troposphere. Nearer the surface, it is more reasonable to consider the mean $O - A$ values
255 (because of subgrid variability in the MOZAIC data), and these indicate that the surface layer
256 forecast errors have substantial spatial variability, and that future improvements to any CO
257 assimilation system would need to take this into account.

258 Assimilation experiments reveal that SCIAMACHY total column observation error standard
259 deviations may be 50 % smaller than the values obtained from the retrieval error estimates. The
260 observation error can be decomposed into random and systematic components. The former rep-
261 resents measurement accuracy and cannot be reduced, while the latter represents the systematic
262 component, and is more likely to be overestimated.

263 The basic driving force behind data assimilation is the observation minus forecast, or $(O - F)$,
264 which represents the difference between the total columns of CO as seen by the satellite and
265 predicted by the model. These $(O - F)$ s represent the sum of forecast and observation errors,
266 without explicit information on which error source predominates, or what level in the atmosphere
267 should be corrected the most. This partition is specified through the error covariance estimates
268 and the averaging kernel. For SCIAMACHY, it results in corrections to the CO field occur at
269 all levels in the troposphere.

270 Over the Arabian Peninsula assimilation of SCIAMACHY data has a large impact on the CO
271 field, which improves comparisons with MOZAIC data (Figure 4). Large model errors in this
272 region motivated sensitivity experiments to investigate their origin. The errors in the CO field
273 relative to MOZAIC data decrease substantially in CO simulation experiments with enhanced
274 CO emissions over the Arabian Peninsula and/or global reduction of OH, indicating that both
275 are important components of the model errors in this region. Even after these changes in the
276 model, the assimilation of SCIAMACHY data further reduces CO errors near the surface by
277 about 50% over Dubai. This indicates the robustness of the beneficial impact of SCIAMACHY
278 data. Other components of the model error that could be investigated in the future include
279 errors in the boundary layer height (which impact mixing of CO into the free Troposphere),
280 parameterization of the convective transport (e.g. Ott *et al.*, 2008) and underestimation of
281 distant or unspecified CO sources (e.g. Kar *et al.*, 2006).

282 Acknowledgments

283 This project was funded in the GMAO under the NASA NRA-03-OES-02 (Carbon cycle
284 research) and a NASA Modeling Analysis and Prediction (MAP) Grant. Computing resources
285 were provided by NASA's High-End Computing Program at GSFC. Funding for the University
286 of Bremen came from DLR-Bonn (grant 50EE0727), ESA (PROMOTE) and the EU-ACCENT-
287 TROPOSAT-2 project. The authors acknowledge the strong support of the European Com-
288 munities, Airbus and the airlines (Lufthansa, Austrian, Air France) who carry the MOZAIC
289 equipment free of charge and have performed maintenance since 1994.

290 References

- 291 Bey, I., D.J. Jacob, R.M. Yantosca, J.A. Logan, B.D. Field, A.M. Fiore, Q. Li, H.Y. Liu,
292 L.J. Mickley and M.G. Schultz, Global modeling of tropospheric chemistry with assimilated
293 meteorology: Model description and evaluation, *J. Geophys. Res.*, Vol 106, pp 23,073-23-95,
294 2001.
- 295 Bloom, S.C., A.M. da Silva, D.P. Dee, M. Bosilovich, J.-D. Chern, S. Pawson, S. Schubert,
296 M. Sienkiewicz, W.-W. Tan, M.-L. Wu, Documentation and Validation of the Goddard Earth
297 Observing System (GEOS) Data Assimilation System (DAS) - Version 4. Technical Report
298 Series on Global Modeling and Data Assimilation 104606, NASA, 26, 2005.
- 299 Bremer, H., J. Kar, J.R. Drummond, F. Nichitu, J. Zou, J. Liu, J.C. Gille, M.N. Deeter, G.
300 Francis, D. Ziskin and J. Warner (2004), The Spatial and Temporal Variation of MOPITT CO
301 in Africa and South America: A Comparison with SHADOZ Ozone and MOIDS Aerosol., *J.*
302 *Geophys. Res.*, 109(D12), D12304, doi:10.1029/2003JD004234.
- 303 Buchwitz, M., I Khlystova, H. Bovensmann, and J.P. Burrows (2007), Three years of global
304 carbon monoxide from SCIAMACHY: comparison with MOPITT and first results related to
305 the detection of enhanced CO over cities, *Atmos. Chem. Phys.*, 7, 2399-2411.
- 306 Cohn, S.E., A. da Silva, J. Guo, M. Sienkiewicz, D. Lamich (1998), Assessing the effects of
307 data selection with the DAO physical-space statistical analysis system, *Mon. Wea. Rev.*, 126,
308 2913-2926.
- 309 Deeter, M.N., L.K. Emmons, G.L. Francis, D.P. Edwards, J.C. Gille, J.X. Warner, B. Khattatov,
310 D.Ziskin, J.F. Lamarque, S.P. Ho, V. Yudin, J.L. Attie, D. Packman, J. Chen, D. Mao, and

311 J.R. Drummond (2003), Operational carbon monoxide retrieval algorithm and selected results
312 for the MOPITT instrument, *J. Geophys. Res.*, *108* (D14), Art No. 4399.

313 Duncan, B.N., J.A. Logan, I. Bey, I.A. Megretskaja, R.M. Yantosca, P.C. Novelli, N.B. Jones and
314 C.P. Rinsland (2007), Global budget of CO, 1988-1997: Source estimates and validation with a
315 global model, *J. Geophys. Res. - Atmos.*, *112*, doi:10.1029/2007JD008459.

316 Guenther, A., *et al.* (1995), A Global-model of natural organic-compound emissions, *J. Geophys.*
317 *Res.*, *100*, pp 8873-8892.

318 Hudman, R.C., *et al.* (2007), Surface and lightning sources of nitrogen oxides over the United
319 States: Magnitudes, chemical evolution, and outflow, *J. Geophys. Res. - Atmos.*, *112*, Art. No.
320 D12S05.

321 Kar, J., J.R. Drummond, D.B.A. Jones, J. Liu, F. Nichitiu, J. Zou, J.C. Grille, D.P. Edwards and
322 M.N. Deeter (2006), Carbon monoxide (CO) maximum over the Zagros mountains in the Middle
323 East: Signature of mountain venting, *Geophys. Res. Lett.*, *33*, L15819, doi:10.1029/2006GL026231.

324 Jacob, D.J., B.D. Field, E.M. Jin, I. Bey, Q. Li, J.A. Logan, R.M. Yantosca and H.B. Singh
325 (2002), Atmospheric budget of Acetone, *J. Geophys. Res. - Atmos.*, *107*, doi:10.1029/2001JD000694.

326 Lahoz, W.A., Q. Errera, R. Swinbank and D. Fonteyn, Data assimilation of Stratospheric con-
327 stituents: a review, *Atmos. Chem. and Phys.*, *7*, 5745-5773.

328 Lamarque, J-F., B. Khattatov, V. Yudin, D.P. Edwards, J.C. Gille, L.K. Emmons, M.N. Deeter,
329 J. Warner, D.C. Ziskin, G.L. Francis, S. Ho, D. Mao and J. Chen (2004), Application of a bias
330 estimator for the improved assimilation of Measurements of Pollution in the Troposphere (MO-
331 PITT) carbon monoxide retrievals, *J. Geophys Res.*, *109*(D16304), doi:10.1029/2003JD004466.

332 Lin, S.J. (2004), A "vertically Lagrangian" finite-volume dynamical core for global models,
333 *Month. Wea. Rev.*, *132*, 2293-2307.

334 Nedelec, P., J.P. Cammas and V. Thouret (1998), Measurement of ozone and water vapor by
335 Airbus in-service aircraft: The MOZAIC airborne program, An overview, *J. Geophys. Res.*,
336 *103*, 25631-25642.

337 Nedelec, P., J.P. Cammas, V. Thouret, G. Athier, J.M. Cousin, C. Legrand, C. Abonne, F.
338 Lecoeur, G. Cayez, and C. Marizy (2003), An improved infrared carbon monoxide analyzer for
339 routine measurements aboard commercial Airbus aircraft: technical validation and first scientific
340 results of the MOZAIC III programme, *Atmos. Chem. Phys.*, *3*, 1551-1564.

341 Ott, L.E., J. Bacmeister, S. Pawson, K. Pickering, G Stenchikov, M. Suarez, H. Huntrieser,
342 M. Loewenstein, J. Lopez, I. Xueref-Remy, An analysis of convective transport and parameter
343 sensitivity in a single column version of the Goddard Earth Observation System, Version 5,
344 General Circulation Model, *J. Atmos. Science*, accepted, 2008.

345 Park, R.J., D.J. Jacob, B.D. Field, BD and R.M. Yantosca (2004), Natural and transboundary
346 pollution influences on sulfate-nitrate-ammonium aerosols in the United States: Implications for
347 policy, *J. Geophys. Res. - Atmos.*, *109*, Art. No. D15204.

348 Parrish, D.D. (2006), Critical evaluation of U.S. on-road vehicle emission inventories, *Atmos.*
349 *Environ.*, *40*, pp 2288-2300.

350 Stajner, I., L.P. Riishøjgaard and R.B. Rood (2001), The GEOS ozone data assimilation system:
351 Specification of error statistics, *Q.J.R. Meteorol. Soc.*, *127*, 1069-1094.

352 Stajner, I., *et al.* (2008), Assimilated Ozone from EOS-Aura: Evaluation of the Tropopause Re-
353 gion and Tropospheric Columns, *J. Geophys. Res.*, *113* (D16), D16S32, doi:10.1029/2007JD008863.

354 Turquety, S., *et al.* (2007), Inventory of boreal fire emissions for North America in 2004:
355 Importance of peat burning and pyroconvective injection, *J. Geophys. Res.*, *112* D12S03,
356 doi:10.1029/2006JD007281.

357 Wang, Y., D.J. Jacob and J.A. Logan, (1998), Global simulation of tropospheric O_3 - NO_x -
358 hydrocarbon chemistry 1. Model formulation, *J. Geophys. Res.*, *103*, 10713-10725.

Carbon Monoxide SCIAMACHY/ENVISAT 2004

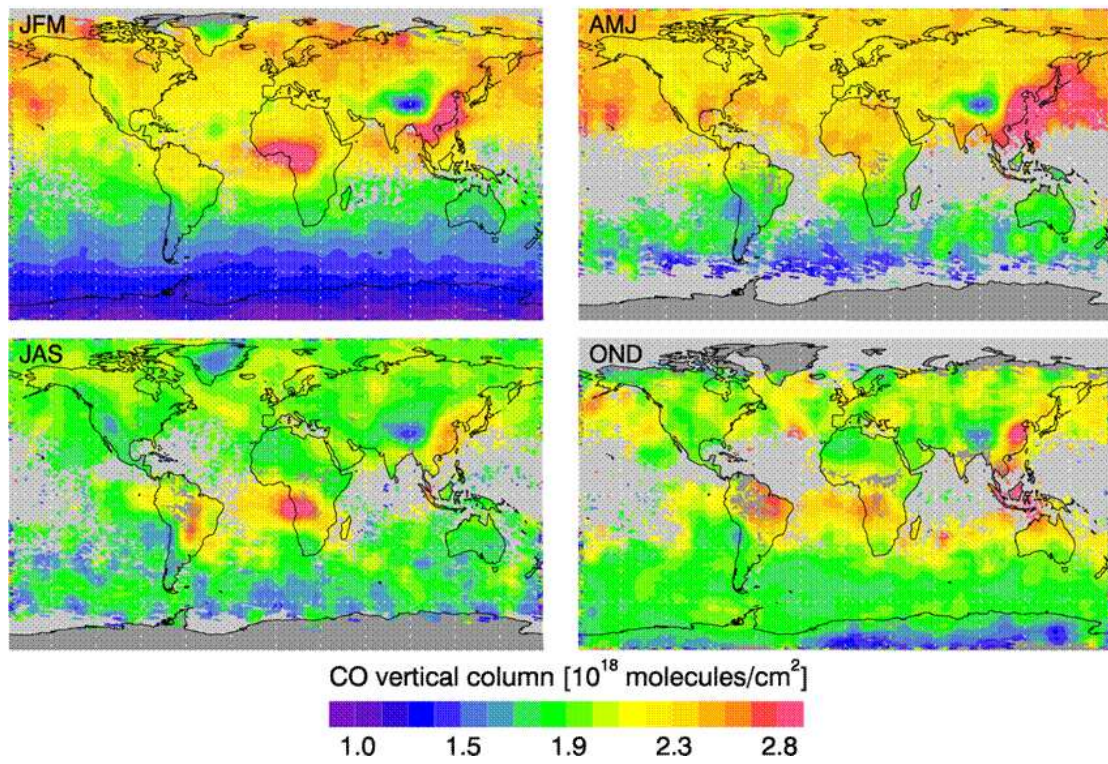
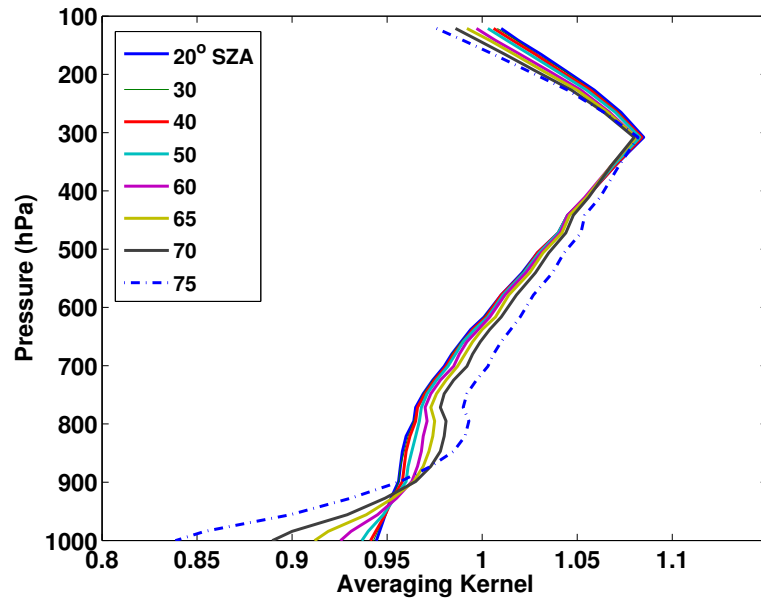
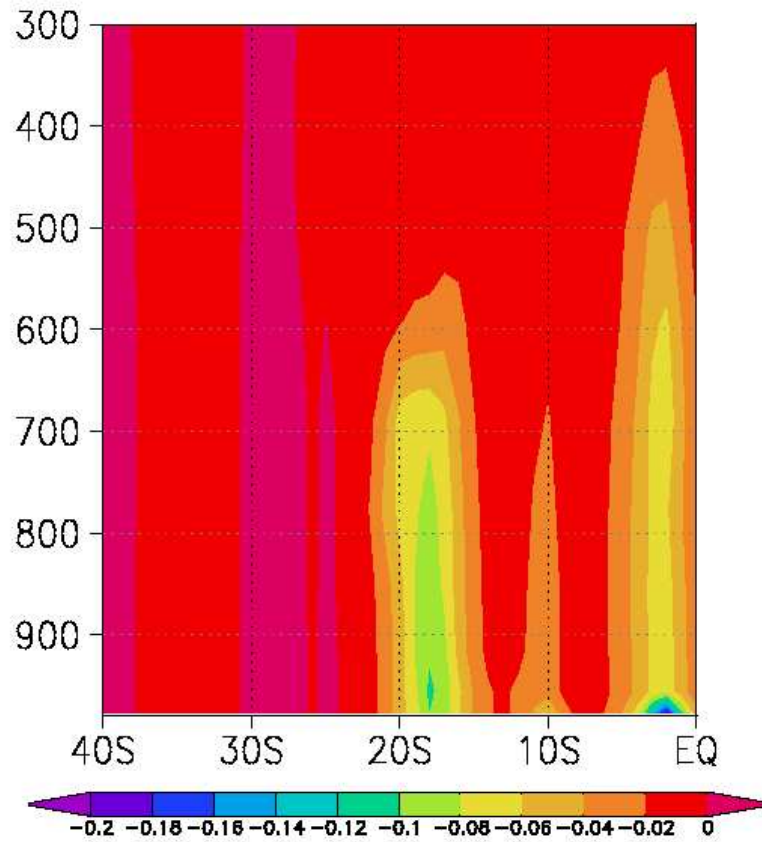


Figure 1: Total Column CO from SCIAMACHY averaged over three month periods during 2004.

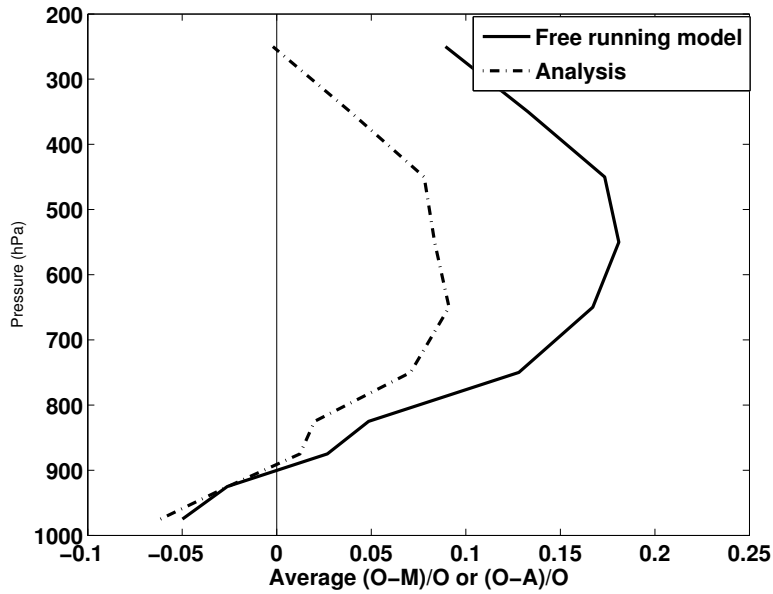


(a)

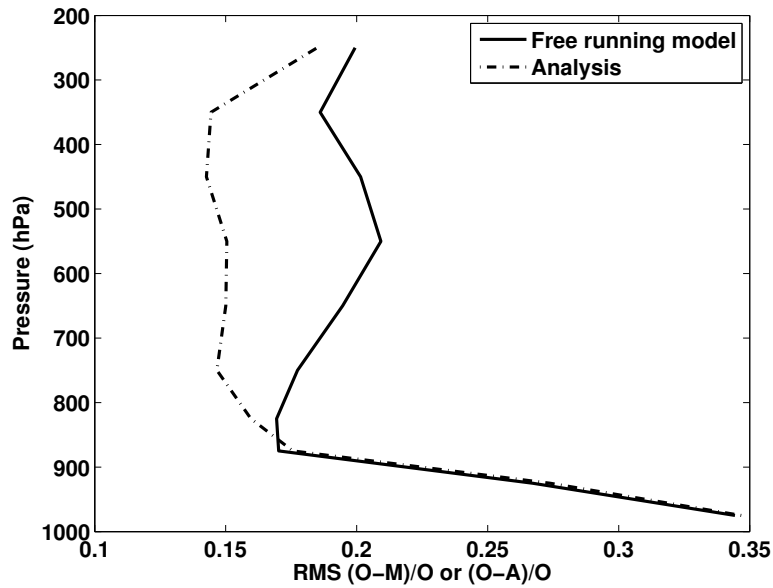


(b)

Figure 2: (a) The SCIAMACHY CO averaging kernel and (b) Analysis increment at 25E over Southern Africa on September 30, 2004. Units are ppmv

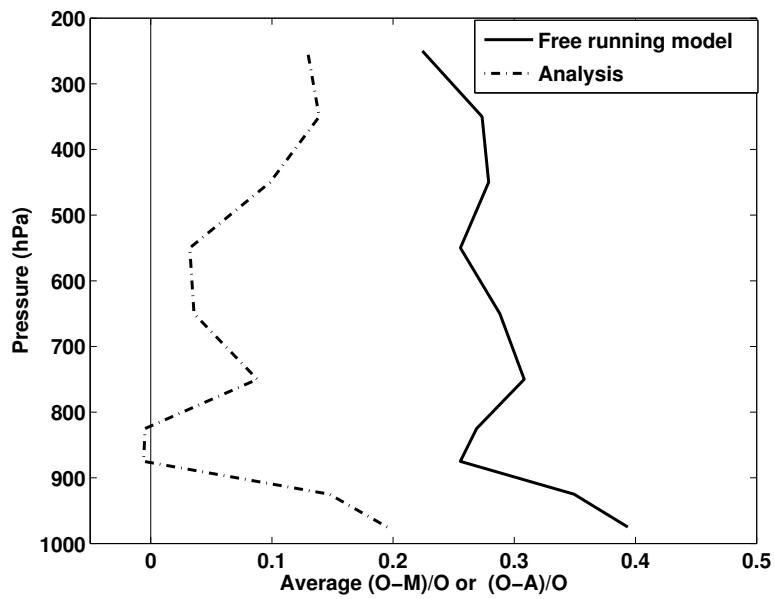


(a)

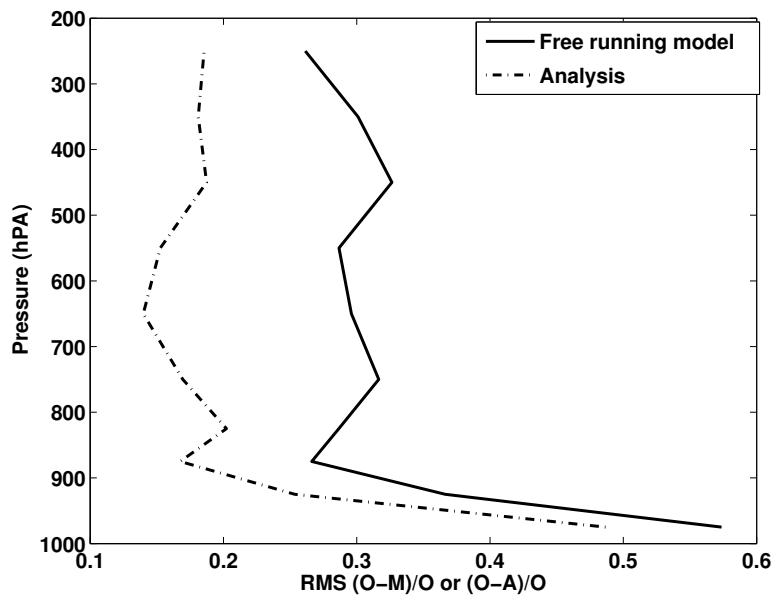


(b)

Figure 3: Relative mean (a) and RMS (b) O-A in the box containing MOZAIC observations within 5 degrees longitude or latitude of Frankfurt, where O refers to the MOZAIC observations, A to the analysis field and M to the CO simulations interpolated to MOZAIC locations. Solid lines refer to the free model run and dash-dot lines refer to the analyses.

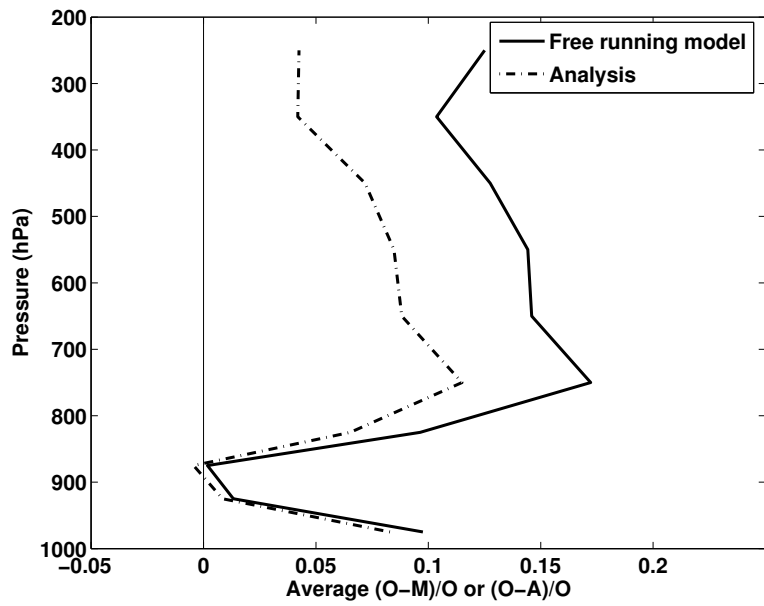


(a)

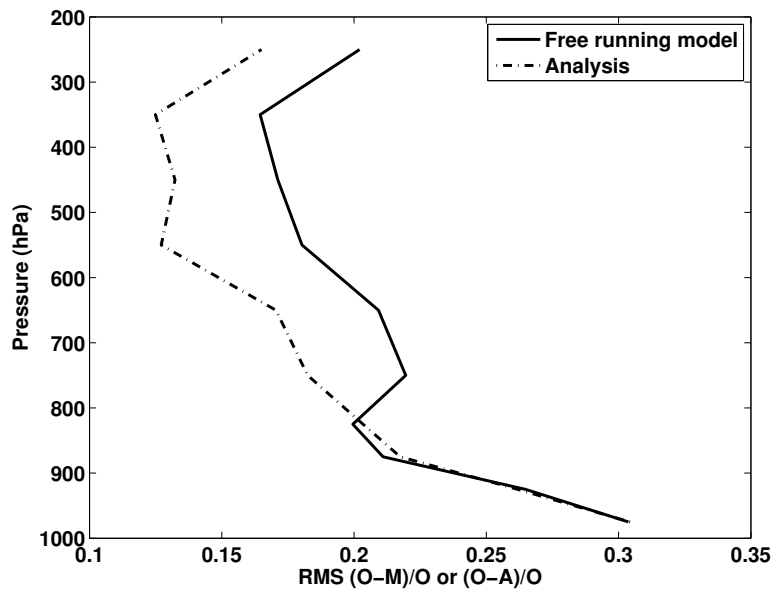


(b)

Figure 4: As in Figure 3 except for Dubai



(a)



(b)

Figure 5: As in Figure 3 except for New York City

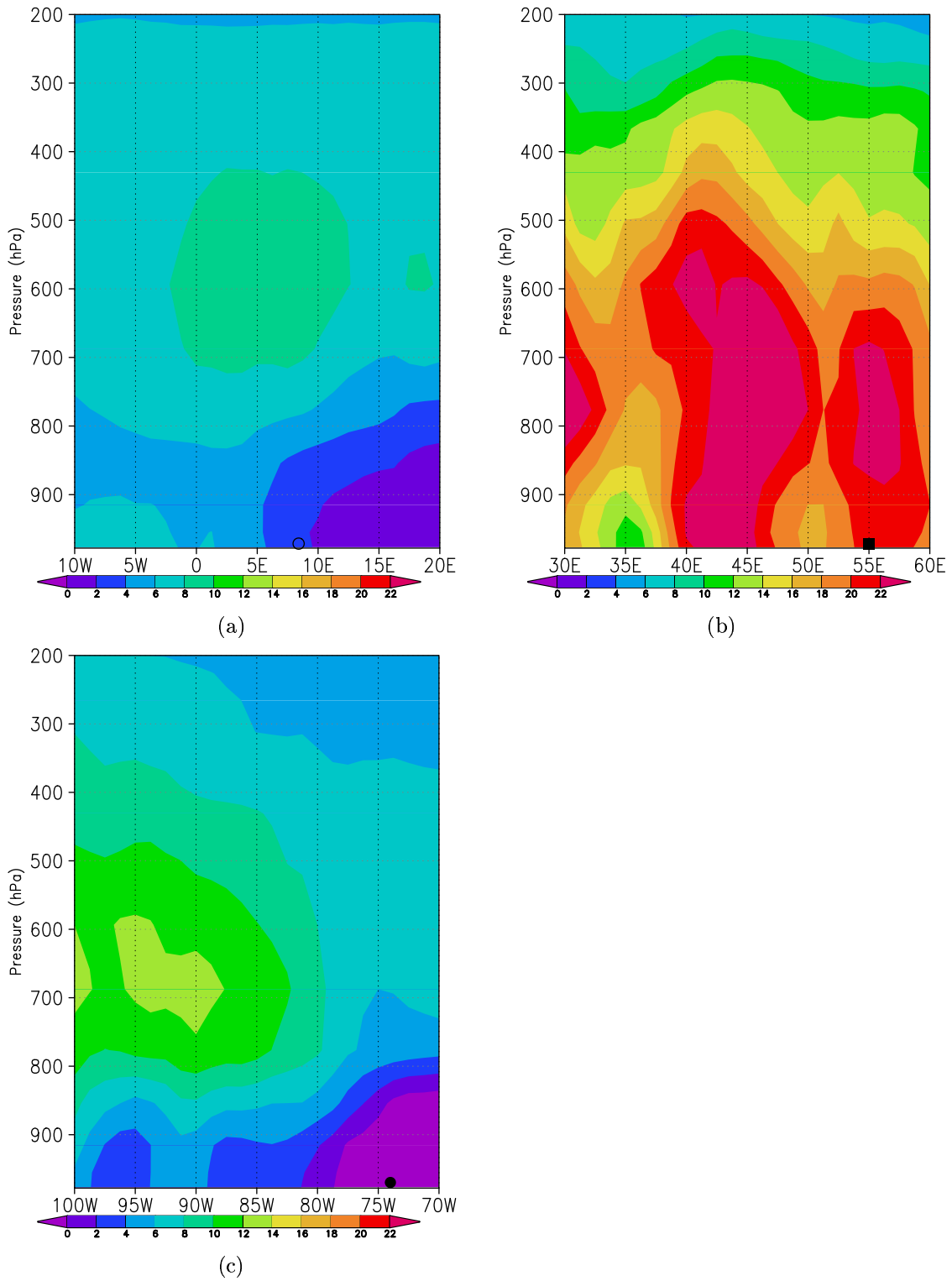


Figure 6: Difference between analysis and free running model in ppbv, averaged over the period September 1 - October 31, 2004 for vertical slices at (a) 51 N, Frankfurt, denoted by open circle; (b) 25 N, Dubai, denoted by square, and (c) 41 N, New York, denoted by solid circle.

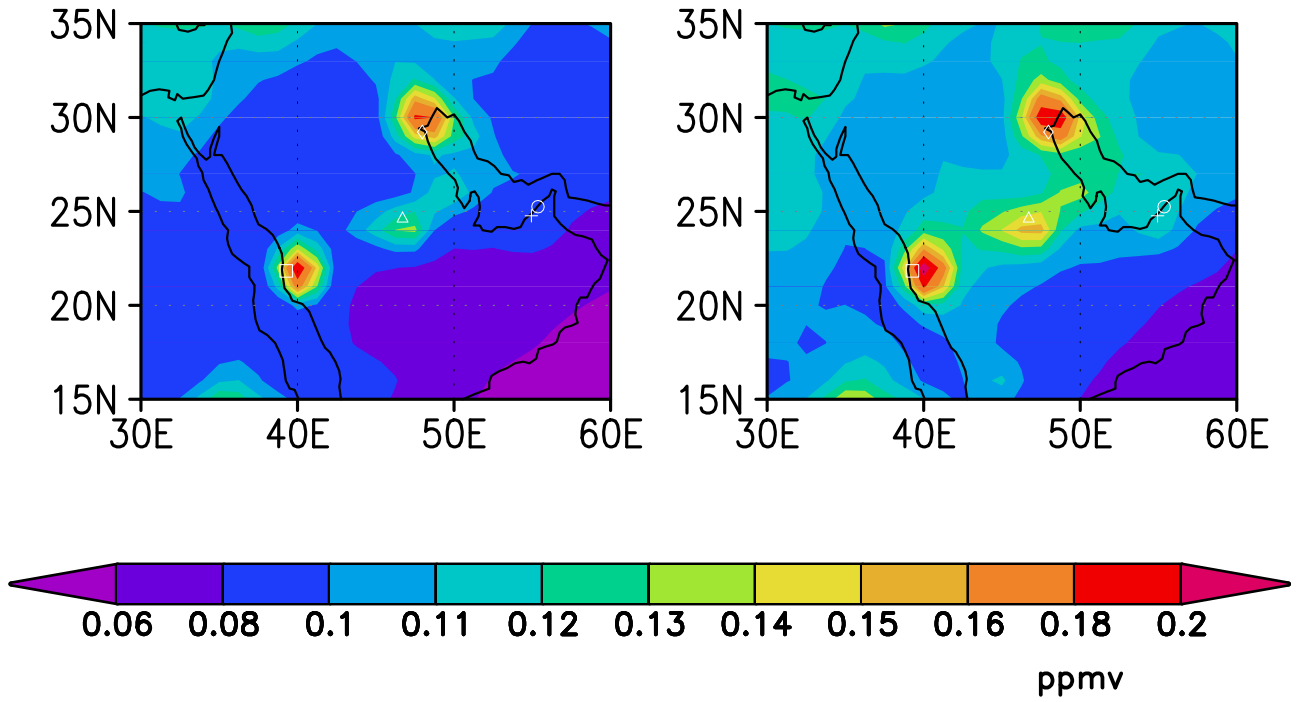
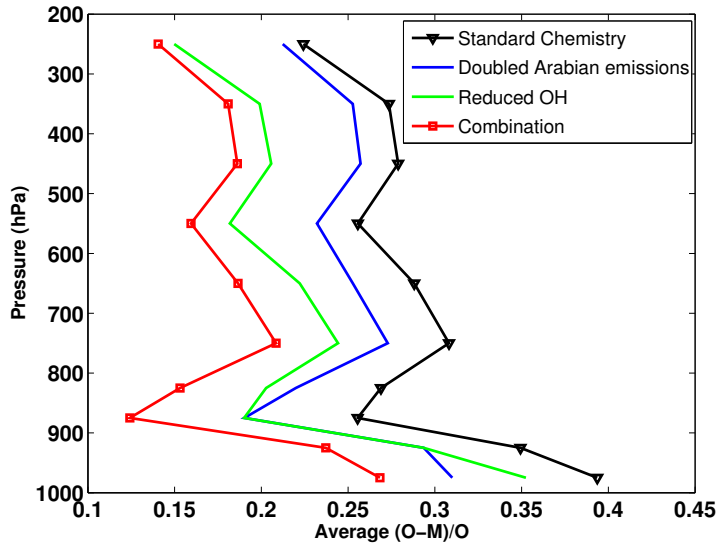
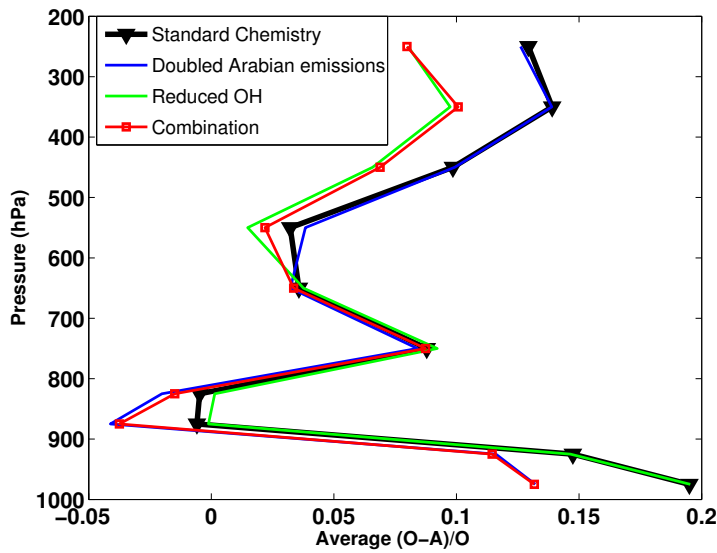


Figure 7: CO field in ppmv for the lowest model layer averaged over the period September 1 - October 31, 2004 for the free running model (left panels) and analysis (right panels) using cloud free observations in the Middle East. The cities marked are Kuwait City (diamond), Jeddah (square), Riyadh (triangle), Abu Dhabi (plus) and Dubai (circle).

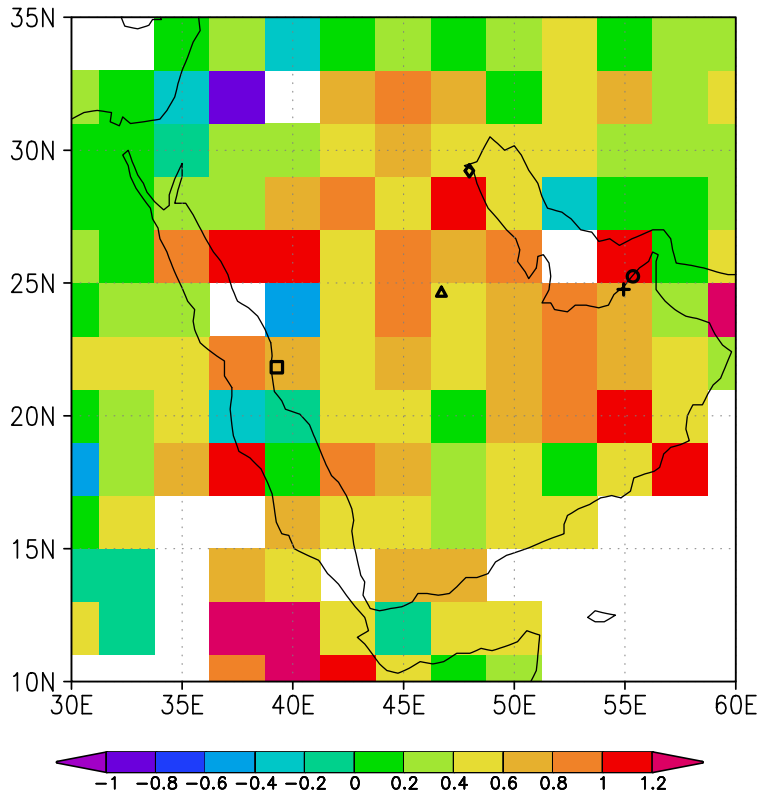


(a)

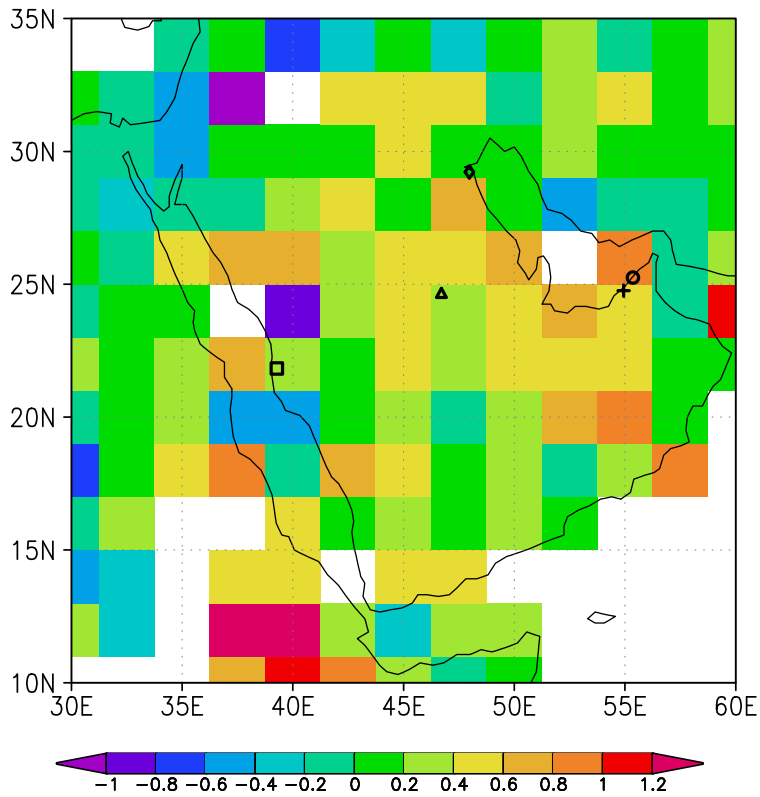


(b)

Figure 8: Relative mean O - M (panel a) and O - A (panel b) in the box containing MOZAIC observations within 5 degrees longitude or latitude of Dubai, where O refers to the MOZAIC observations, M refers to the free model run and A is the analysis field interpolated to MOZAIC locations. The black lines (with triangles) use the standard (GEOS-CHEM) anthropogenic emissions, the blue lines use a chemistry model with doubled CO emission in the Arabian peninsula, the green lines contain a 10% global reduction in OH and the red lines (with squares) use both model adjustments.



(a)



(b)

Figure 9: Total Column observed minus (O-F) values ($molecules/cm^2/1.0 \times 10^{18}$) averaged over the month of October 2004, for the Arabian Peninsula using standard chemistry (a) and using doubled Middle East emissions and a global 10% reduction in OH (b). Symbols for cities are the same as in Figure 7.

Assimilation of SCIAMACHY total column CO: Regional analysis of data impact

Tangborn, A., I. Stajner, M. Buchwitz, I. Khlystova,
J. Burrows, S. Pawson, R. Hudman, P. Nedelec

Abstract

Carbon monoxide (CO) total column observations from the SCanning Imaging Absorption SpectroMeter for Atmospheric CHartographyY (SCIAMACHY) on board ENVISAT are assimilated into the Global Modeling and Assimilation Office (GMAO) constituent assimilation system for the period July 18-October 31, 2004. This is the first assimilation of CO observations from a near infrared sounder. The impact of the assimilation on CO distribution is evaluated using independent Measurement of Ozone and Water Vapor by Airbus In-service Aircraft (MOZAIC) *in situ* CO profiles. Assimilation of satellite data improves agreement with MOZAIC CO globally, especially in the upper troposphere. Regional comparisons are made in western Europe, the northeastern United States and the Arabian Peninsula. SCIAMACHY assimilation improves CO mixing ratios at pressures ≤ 800 hPa in all three locations. In contrast, the only substantial planetary boundary layer improvements occur over the Arabian Peninsula, with mean error reduction of 50%.

Model errors (sources and chemistry) are investigated through experiments with increased surface CO emissions over the Arabian Peninsula and/or globally reduced hydroxyl radical (OH) concentrations. Both model changes decrease mean errors at all altitudes in the free running model in comparison to MOZAIC data over Dubai and Abu Dhabi. In contrast, errors in the assimilated CO are reduced by the increased emissions only near the ground for pressures ≥ 800 hPa and by the reduced OH only for pressure ≤ 600 hPa. Our analysis suggests that CO emissions over Dubai in 2004 are more than 100% larger than those in the 1998 emissions inventory.